Aerosol and Air Quality Research, 14: 1392–1401, 2014

ISSN: 1680-8584 print / 2071-1409 online
doi: 10.4209/aaqr.2013.11.0336

Microstructure and Chemical Composition of Diesel and Biodiesel Particle Exhaust

Olga B. Popovicheva[1*], Elena D. Kireeva[1], Sandro Steiner[2], Barbara Rothen-Rutishauser[2], Natalia M. Persiantseva[1], Mikhail A. Timofeev[1], Nataljia K. Shonija[1], Pierre Comte[3], Jan Czerwinski[3]

[1] *Skobeltsyn Institute of Nuclear Physics, Lomonosov Moscow State University, Leninskie Gory1, 119991, Moscow, Russia*
[2] *Adolphe Merkle Institute, University of Fribourg, Route de l' ancienne Papeterie 1723 Marly, Fribourg, Switzerland*
[3] *Division of Automotive Engineering, Bern University of Applied Science, AFHB Abgasprufstelle Gwerdstr.5, CH-2560, Nidau, Switzerland*

ABSTRACT

The complexity and large variability of transport-emitted aerosols leads to necessity of comprehensive characterization of their physico-chemical and toxicological properties, remaining great uncertainties in health effect assessments. Particles produced by combustion of fossil diesel (B0), 20% rapeseed methyl ester in fossil diesel (B20), and pure rapeseed methyl ester (B100) were sampled from exhaust of an Opel Astra diesel engine using sulfated ash, phosphorous and sulfur (SAPS) lube oil with low and high ash content. Microscopic and chemical characterization is performed to quantify the common and specific properties of diesel/biodiesel exhausts. Hydrophobic saturated aliphatic dominate diesel particle chemistry. Oxygen and nitrogen-containing functionalities are specific for more hydrophilic biodiesel particles. A full range of chemical species for individual particles is grouped by clustering technique combined with water-soluble ion measurements. Analysis of group abundance shows carbonaceous particles (soot externally mixed with inorganic salts) and inorganic fly ash (metal oxides) in a structure of exhaust, in correlation with inorganic contaminations in fuel and lube oil. Quantification of particle types in terms of physicochemical relevance supports the identification of groups which may act as biomicromarkers discriminating between diesel and biofuel exhaust and micromarkers of using high ash lube oil, thus providing a basis for correlative toxicological assessment of diesel/biofuel engine emissions.

Keywords: Combustion particles; Diesel exhaust; Aerosols.

INTRODUCTION

Combustion aerosols are the ubiquitous substance that is produced by incomplete burning of fossil fuels and biomass. Transport activities contribute 20–25% of total anthropogenic emission of carbonaceous particles (Cofala *et al.*, 2007). In Europe more than 70% of carbonaceous aerosols originate from the transport sector. The composition of combustion aerosols significantly impacts air quality, radiative balance, and climate (Chow and Watson, 2011). Investigations of their physico-chemical properties are gaining importance due to enhancement of air pollution reduction relating to improvement of engine performance, fuel efficiency, and after-treatment strategies.

Currently diesel exhaust particles are gaining an increasing attention because of pronounced impacts on human health (Donaldson *et al.*, 2005). They are considered as dangerous pollutants because of high number density, small respirable size, large surface area, and potential toxicity. Particle toxic potential has been associated with serious adverse health effects, including respiratory symptoms impaired lung function and cardiovascular diseases (Geller *et al.*, 2006; Bernstein *et al.*, 2004). It is found that newer diesel engines emit nanoparticles that could be more harmful to human health than older engines because particles with diameters of 5–20 nm may penetrate the lung more deeply (Su *et al.*, 2008).

Diesel soot emitted by modern engines demonstrates defective surfaces with chemically reactive sites which destabilizes the carbon structure and may increase soot cytotoxicity. InfraRed studies show a high concentration of hydroxyl functional groups on Euro IV soot compared to soot emitted by older engines (Su *et al.*, 2008), and hence an increased hydrophilicity which facilitates interactions

* Corresponding author.
Tel.: 1-513-558-0504; Fax: 1-513-558-2263
E-mail address: polga@mics.msu.su

with hydrophilic biomolecules (Popovicheva *et al.*, 2009a). Based on inflammatory and cytotoxic responses to in vitro and in vivo particle exposures, the hazardous substances are found on particles emitted by various vehicles but risks associated to chemical forms of these emissions are remaining uncertain (Maier *et al.*, 2008; Muller *et al.*, 2010). Due to a lack of characterization data the current practice for assessing effects of diesel-produced particles on air quality is based largely on the quantity of emitted particles and their size, and limited on their chemical composition and toxicological properties.

Since the particle formation depends on several factors, e.g., type of fuel and engine operation conditions, their morphology and composition varies considerably. Carbonaceous components of fossil fuel-derived particulate matter contain ultrafine soot agglomerates with fractal chain morphology and spherical primary particles between 30 and 50 nm in diameter (Chen *et al.*, 2005). A basic feature of soot is the elemental carbon microstructure of graphite microcrystallites (Popovicheva *et al.*, 2003; Vander Wal *et al.*, 2007). Unburned organic components and inorganic contaminations in fuel, lube oil, and engine wear are condensed on soot particles in chemical forms of organic carbon (OC) and inorganic fly ash that together comprise extremely complex exhaust structure (Kleeman *et al.*, 2000; Sakurai *et al.*, 2003; Toner *et al.*, 2006). The OC content varies with engine operating conditions and can represent 5–90% of total particulate mass dominated by alkanes, hopanes, steranes, and polyaromatics (Chow *et al.*, 2007). Single particle characterization of heavy duty diesel emission demonstrates that particles made from elemental carbon (EC), OC, Ca, and phosphates are dominating (Toner *et al.*, 2006). The increase of engine speed results in increased metal content of crustal origin (Wang *et al.*, 2003). All conventional piston-driven combustion engines emit metal oxide particles produced in nucleation processes during combustion due to abrasion, catalyst coatings, metal-organic lube oil and fuel additives (Mayer *et al.*, 2010).

Fatty acid methyl esters (FAMEs), also referred as biodiesel, are oxygenated fuels made from vegetable oils and animal fats via transesterification. They have long been recognized as reducing the exhaust particle mass and number as compared to diesel fuel (Jung *et al.*, 2006; Betha and Balasubramanian, 2011). The increase in consumption of biodiesel blend fuels led to changes in diesel pollutant emission (Singh and Singh, 2012) including changes of physico-chemical properties of the emitted particles, their size (Jung *et al.*, 2006), the soluble organic fraction (Dwivedi *et al.*, 2006), and metal content (Dwivedi *et al.*, 2006; Betha and Balasubramanian, 2011). Health risk estimates based on exposure and dose-response assessments of particulate-bound elements revealed that biofuel exhaust is more hazardous (Betha and Balasubramanian, 2011).

There are strong indications of particle biological activity in dependence on physico-chemical characteristics, which are not considered in many toxicity studies (Oberdorster *et al.*, 2005). Risk assessment of diesel exhaust emissions was done by exposing the exhaust directly to the surface of lung cells cultured at the air-liquid interface (Steiner *et al.*, 2012). A complex three dimensional cellular model of the human lung epithelium was used to present the lung cells (Rothen-Rutishauser *et al.*, 2008; Muller *et al.*, 2010). Volatile and soluble organics content are found to be higher in biodiesel exhaust compared to standard diesel (Dwivedi *et al.*, 2006). Diesel particles contain substantially more PAHs than rapeseed oil while carcinogenic PAH level is higher for rapeseed oil exhaust (Topinka *et al.*, 2012).

The effects of inhaled aerosols at the cellular level depend on both their size and distribution of toxic components over particles. Most diesel exhaust studies have aimed to obtain the information on average chemical characteristics by bulk analytic techniques while characterization of individual particles is significant for health impact assessment as providing the chemical composition and morphological information at the microscopic level. Single particle analysis reveals the particle types to present the major signatures in exhaust (Toner *et al.*, 2006). Scanning Electron Microscopy (SEM) coupled with Energy-dispersive X-ray Spectroscopy (EDX) is a powerful tool for characterization of size, morphology, and composition of individual particles in combustion emissions (Chen *et al.*, 2005, 2006; Vester *et al.*, 2007; Kireeva *et al.*, 2009). Characterization of multicomponent diesel exhaust previously was done in accordance with morphological specification, such as soot-like, char, and mineral particles (Chen *et al.*, 2005; Popovicheva *et al.*, 2009b). However, cluster analysis is presently well-developed multivariate data analysis technique useful for interpretation of electron microprobe analysis data (Popovicheva *et al.*, 2012). The range of similar species in exhaust may be grouped revealing the particle types according to morphology and composition. With this purpose bulk analytic techniques are useful to identify inorganic compounds and ions in the diesel engine exhaust.

This paper is devoted to characterization of microstructure and chemical composition of particle exhaust produced by Opel Astra X20DTL engine using diesel and biodiesel, and lube oil of different purity (low and high SAPS). The individual particle analysis is performed by SEM/EDX to determine the morphology and composition of aerosols produced at controlled combustion conditions. For classification of individual particles and quantification of structure of the exhaust the cluster analysis is performed. Expert analysis based on water-soluble inorganic ion measurements is applied for interpretation of clustering data and best separation on characteristic groups. Micromarker of using high SAPS lube oil and biomicromarker of biodiesel using are identified. Results of characterization are discussed together with toxicological responses of human lung cells exposed by B0, B20 and B100 exhaust at the air liquid interface, including cell death, induction of oxidative stress, and pro-inflammatory responses.

EXPERIMENTAL

An Opel Astra X20DTL was running on a dynamometer at a constant velocity of 35 km/hr with a force of 66N at the wheel. The test vehicle was a 4 cylinder Diesel engine, 1994 cc displacement, production year 1998 and 70000 km

mileage. This vehicle was little used and at normal technical state without excessive oil consumption. Conventional diesel fuel DIN EN 590 (B0) of swiss market quality, a blend of 80% fossil diesel and 20% rapeseed methyl ester (B20), and pure fatty rapeseed methyl ester (B100) were used as fuels. Sulfur content in B0 and B100 is 10 and 5.2 mg/kg. Ca, K of 5.6 and 3.4 mg/kg are found in B100. V10.237 and V10.240 sulfated ash, phosphorous and sulfur (SAPS) contained high and low ash of 1.5 wt% and < 0.7 wt%, respectively, were used as lube oil. Composition of ash is dominated by Ca, S, and Zn content.

Sampling of total suspension particles was performed with a CVS system at B0 low and high SAPS, B20 high SAPS, and B100 high SAPS conditions. For particle sampling fluorocarbon-coated borosilicate glass fiber filters (T60A20, Pall Life Sciences) were used. Sampling was repeated three times for each from four conditions to estimate the combustion variability impact on particle properties.

The particle chemical composition was analyzed by Fourier Transform Infrared (FTIR) spectroscopy using a Shimadzu IRPrestige-21 spectrometer in a transmission mode. FTIR spectra are measured at 4 cm^{-1} resolution. Each spectrum was an average of 100 scans in the typical wavenumber range from 4000 to 500 cm^{-1}. IRSolution (Shimadzu) software was used to subtract the spectrum of a blank filter from the spectrum of the loaded filter, and to correct the baseline absorbance. The scaled subtraction was performed by the spectrum normalization on a band at 1400 cm^{-1}. The difficulty in completely subtracting out the strong blank filter absorption in the region of 1200–800 cm^{-1} reduces the usefulness of analysis in this region. Moreover, the spectra of sample filters do not demonstrate any absorbance bands in the region of 800–450 cm^{-1}. This is why all following spectra interpretation is done in the region of 3600–1250 cm^{-1}. Identification of absorption bands is carried out according to a FTIR database (Lin-Vien *et al.*, 1991; Coates, 2000) and measurements of standard compounds.

Water-soluble inorganic ion mass concentrations were measured using a capillary electrophoresis (CE) system (Capel-103, Lumex Corp.). Six anions (SO_4^{2-}, NO_3^-, Cl^-, F^-, NO_2^-, and PO_4^{3-}) and six cations (Na^+, NH_4^+, K^+, Mg^{2+}, Sr^+, and Ca^{2+}) were determined in aqueous extracts. One-forth filter sample was extracted in 5 ml of distillated water by ultrasonic agitation for 30 min, and then the extract was filtered. CE methodic details are described elsewhere (Kaniansky *et al.*, 1999). Because large contaminations of blank filters T60A20 by NH_4^+, Na^+, K^+, Cl^- the measurement error (std) for these ions were high, in the range from 39 to 66%. For other ions SO_4^{2-}, Ca^{2+}, Ba^+, Cl^-, NO_3^- it was 49, 50, 39, 46, 34%, respectively.

Individual particles were examined using the LEO 1430-vp (Karl Zeiss) field emission scanning electron microscope with a spatial resolution of 7 nm equipped with an Oxford energy dispersive detector INCA. Energy dispersive X-ray spectroscopy spectra for Z elements ($Z \geq 5$) were recorded in SEM image mode and then quantified by means of a method that relates the measured X-ray intensity to the elemental concentration, using calculated equivalent X-ray intensities of corresponding elements. Counting time for X-ray spectra was 50 seconds at 5.9 kV. Particles from the sample filters were removed onto Cu substrate by ultrasonic treatment during 30 min. Approximately 500 fine individual particles with a diameter from 0.1 up to 3 μm were chosen for each sample, a number sufficient to get certain types of particles in the each sample (Chen *et al.*, 2006; Popovicheva *et al.*, 2012). Significantly larger sizes were not considered because relating to coarse agglomerates. Small concentrations of C and O in the substrate were subtracted from the EDX spectra of analyzed particles.

The result of EDX analysis was a data matrix of 20 element weight concentrations. Combination of hierarchical and non-hierarchical cluster analysis, k-means and g-means, was applied to separate individual particles in definable groups of similar chemical composition using software Deductor. More details are described elsewhere (Bladt *et al.*, 2012; Popovicheva *et al.*, 2012). The justification for the number of groups of the best separation is the identification of different chemical particle types. In this case the clustering with lower number of groups does not provide a good separation while a higher number leads only to duplication of groups with similar composition.

RESULTS AND DISCUSSION

Chemical Composition

FTIR analysis gives a good overview of exhaust particle chemical composition. Fig. 1 shows representative FTIR spectra of particles produced at B0 low and high SAPS, B20 high SAPS, and B100 high SAPS conditions. The observation of high similarity for FTIR spectra of samples repeatedly produced at the same condition reveals a high reproducibility of engine operation. The most intensive spectral feature for all emissions is bands of aliphatic C-C-H stretch vibrations of alkyl groups in alkanes. Strong asymmetric and symmetric stretches of methylene CH_2 groups are observed at 2924 and 2853 cm^{-1}, respectively. An asymmetric stretch of methyl CH_3 groups is slightly prominent at 2951 cm^{-1} as a weak shoulder of a much stronger CH_2 asymmetric stretch. The bands at 1456 and 1375 cm^{-1} are assigned to asymmetric and symmetric bend vibrations of methyl alkyl groups. There is a difference in composition between low and high SAPS for any fuel used due to a wide band in the region of 1517–1533 cm^{-1} associated to aromatic -NO_2 vibrations but for diesel fuel it is very slightly prominent.

The band of carbonyl C=O stretch vibrations in the range of 1718–1753 cm^{-1} is related to carboxylic acids, ketones, aldehydes, esters, and lactones. It is the most significant for B100 high SAPS than for B20 high SAPS, relating to higher carbonyl production in biofuel exhaust (Karavalakis et al, 2011). As a peak area of FTIR band is assigned to abundance of functionalities, a higher ratio of carbonyl C=O to aliphatic C-C-H band indicates more hydrophilic character of the surface for B100 than for B20 particles.

In the region of 580–680 cm^{-1} relatively significant vibrations of SO_4^{2-} ions are indentified, they are produced due to sulfur contaminations either in fuel or oil. While

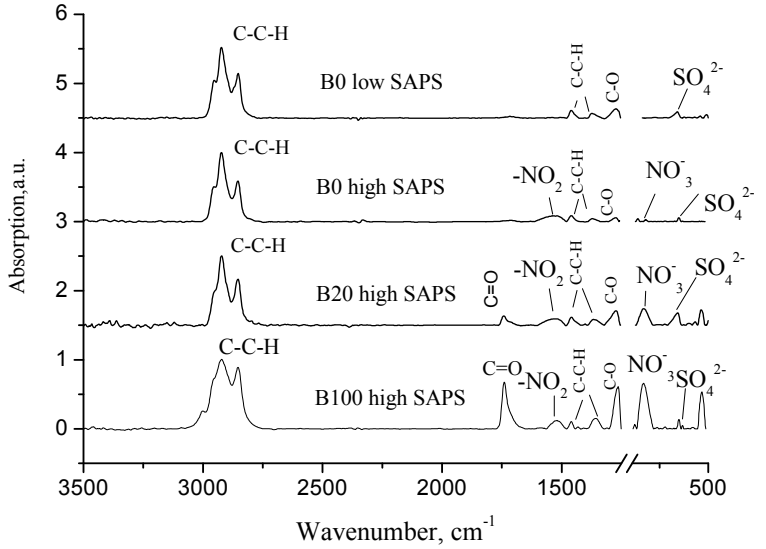

Fig. 1. FTIR spectra of particles produced at B0 low and high SAPS, B20 high SAPS, and B100 high SAPS conditions.

slightly prominent NO_3^- ion vibrations are observed at 833 cm^{-1} for B0 high SAPS, they are more significant for B20 and B100 high SAPS, relating to higher nitrification of the particle surface in the biofuel exhaust. Also, in last case the band in the region of 1357–1365 cm^{-1} is associated to NO_3^- vibrations.

Mass concentrations of water-soluble inorganic ions in diesel and biodiesel exhaust particles are shown in Fig. 2. Na^+, Ca^{2+}, NO_3^-, K^+, Ba^+, and Cl^- ions account for more abundant ionic species in all exhausts. NO_3^- ions dominate at high SAPS for any fuel used, well in accordance with FTIR data, its maximum concentration approaches 1.0% of particulate mass. In comparison with low SAPS exhaust, higher concentrations of Ca^{2+} and SO_4^{2-} ions are observed at high SAPS, in accordance with elevated ash content in high SAPS. Variable concentrations of ammonium, potassium, sodium, calcium, and chloride as well as sulfates and nitrates ions indicate the presence of water-soluble salts in diesel/biodiesel particles.

Individual Particle Analyses

Individual particle analysis reveals the complex structure of aerosol exhaust produced by an Opel Astra engine. SEM/EDX observations show carbonaceous particles internally and externally mixed with inorganic compounds. The composition of individual particles is varying in a wide concentration range of common (C, O) and trace elements representative fuel and lube oil content. Groups of particles identified at B0 low and high SAPS, B20 high SAPS, and B100 high SAPS conditions and their abundances are presented in Table 1. Using the cluster analysis of the chemical composition combined with morphological information it is reasonable to propose the group identification according the chemical particle types.

Soot particles are formed via vaporization-condensation of fuel hydrocarbons during combustion. In accordance with specific features of soot they are typically observed for diesel emissions (Clague *et al.*, 1999; Miller *et al.*, 2007; Kireeva *et al.*, 2009). Group Soot composes the major part

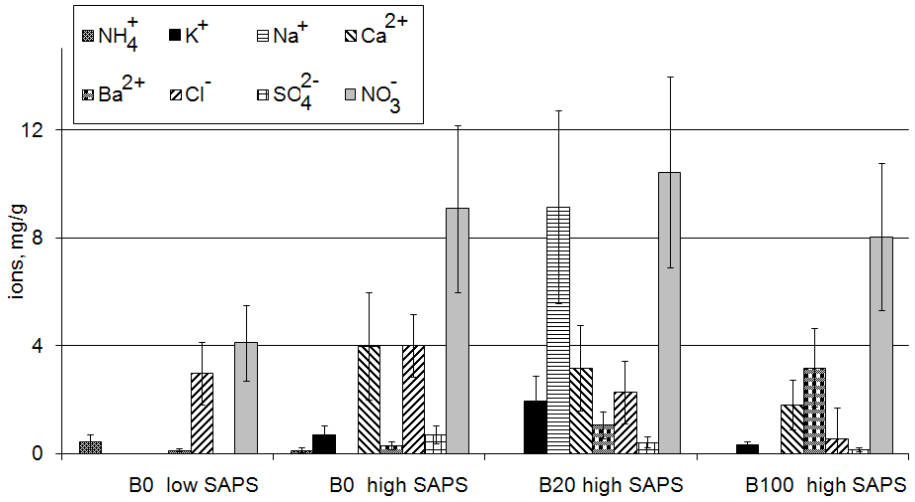

Fig. 2. Inorganic ions in particles produced at B0 low and high SAPS, B20 high SAPS, and B100 high SAPS conditions.

Table 1. Groups, abundance, major elements with averaged composition, and types of particles.

group	types of particles	B0 low SAPS	B0 high SAPS	B20high SAPS	B100 high SAPS
Carbonaceous particles					
Soot	soot	$C_{78}O_{13}$ (42.5)**	$C_{90}O_8$ (50.6)	$C_{83}O_{15}$ (44.6)	$C_{87}O_{10}$ (47.7)
Ca-rich	oxide/carbonates/sulfates	$C_{34}O_{39}Ca_{24}$ (8.7)	$C_{28}O_{49}Ca_8Si_2S_3Mg_3$ (12.5)	$O_{30}C_{45}Ca_{18}$ (11.4)	$C_{34}O_{33}Ca_{26}S_4$ (20.0)
Na, Cl, K- rich	chlorides	no biomicromarker	no biomicromarker	$C_{52}Na_{15}O_{13}$ $Cl_9K_7N_2$ (5.9)	$C_{65}O_{15}K_7$ Cl_5Na_2 (6.2)
Si-rich	oxides	$C_{15}O_{50}Si_{21}Fe_6K_4$ (21.5)	$C_{17}O_{54}Si_{21}Al_2Fe_2$ (8.1)	$O_{32}C_{52}Si_{13}$ (4.1)	$C_{33}O_{37}Si_{16}Al_3Cl_2Ca_4$ (12.8)
Fly ash - bearing particles					
Fe-	oxides	$Fe_{56}O_{28}C_{14}$ (21.0)	$Fe_{50}O_{23}C_6Ni_{12}$ (9.4)	$Fe_{60}O_{23}C_{13}Cl_4$ (9.8)	$Fe_{46}C_{20}O_{28}Ca_4$ (3.6)
Al-	oxides	$Al_{48}O_{43}C_{10}$ (6.6)	$Al_{35}C_{16}O_{48}$ (8.1)	$O_{32}Al_{27}C_{39}$ (4.6)	$C_{57}O_{24}Al_{13}Si_3$ (2.9)
Nb-, Zn-,S-	oxides/sulfates		$Nb_{59}C_{12}O_{27}$ (6.2)	$Zn_{70}C_{12}O_{14}$ (6.2)	$C_{65}O_{15}S_{15}Na_2Ca_3$ (6.6)
W-	oxides		$W_{90}C_9$ (5.0)	$W_{80}O_{15}C_4$ (9.3)	

* average group composition (wt%), more than 1 wt%.
** group abundance (%) is indicated in bracket.

of carbonaceous particles in all exhausts; it consists of chain agglomerates with morphology of primary roughly spherical particles of diameter from 20 to 50 nm. In average, soot contain mostly C and O with a negligible amount of other impurities (< 2 wt%). The agglomerate size ranges from 100 nm to 1 μm.

In Group Ca, Si, and Na, Cl, K-rich these elements are most abundant after carbon and compose fly ash internally/ externally mixed in carbonaceous matrix. Groups Fe-, Al-, Zn-, Nb-, W- bearing are identified according to the content of major element higher than C which determines the particle type. All these groups contain irregular shaped particles in a size range > 200 nm. They are formed during decomposition, subsequent oxidation, and nucleation of contaminations in fuel and lube oil. The formation of coarse particles (> 1 μm) can be explained by coalescence of molten grains of minerals in fuel during combustion while that of submicrometer particles occurs by a vaporization-condensation mechanism (Lighty, 2000). The abundance of elements over individual particles, other than C and O, is shown in Fig. 3. As seen, Ca, Si, Al, and Fe are the most abundant for all emissions studied, and they compose the separated groups.

For diesel B0 low SAPS the clustering of the particles on five groups gives the best separation. For demonstration of element variability the group average composition and standard deviation are presented in Table 2. Representative SEM micrographs of B0 low SAPS groups are shown in Fig. 4. The most abundant is Group Soot composed from well-fused primary soot particles. Particles of Group Si-bearing are mostly quartz because the large amount of O and angular chips shape found for SiO_2 particles formed during combustion. However, small amount of Al accompanies Si in one third fraction of particles in this group, relating to various aluminum silicates. Group Fe-rich is dominated by Fe and O associated with the irregular shaped iron particles, observed in Miller *et al.* (2007). They typically originate from engine wear and corrosion, and presented by iron oxide (Bladt *et al.*, 2012). Group Ca-rich is probably a mixture of calcium carbonate ($CaCO_3$) and calcium oxide (CaO). Some amount of S observed may allow suggesting the presence of calcium sulfates, in correlation with sulfates ions measured. Group Al-bearing is composed of aluminum oxide because of large O content and morphologically well-formed crystals.

Relating to elevated abundance of P, Al, W, Ni, Nb, Mg, Zn, S, and Ti over particles at high SAPS, Fig. 3, we conclude the impact of contaminations in lube oil on the particle composition. Representative micrographs for groups of diesel B0 high SAPS are shown in Fig. 4. Using lube oil of high ash content leads to decreasing of Si and Fe oxide particle groups for diesel B0 high SAPS while the most prominent result is the appearance of Group Nb- and W-bearing composed from niobium oxide and tungsten particles, respectively. Thus, we may relate Groups Nb- and W-bearing as micromarkers of using of high SAPS lube oil.

For biodiesel B20 exhaust structure the clustering reveals the similar groups of soot externally mixed with inorganic salts and metal oxides as for diesel one. However,

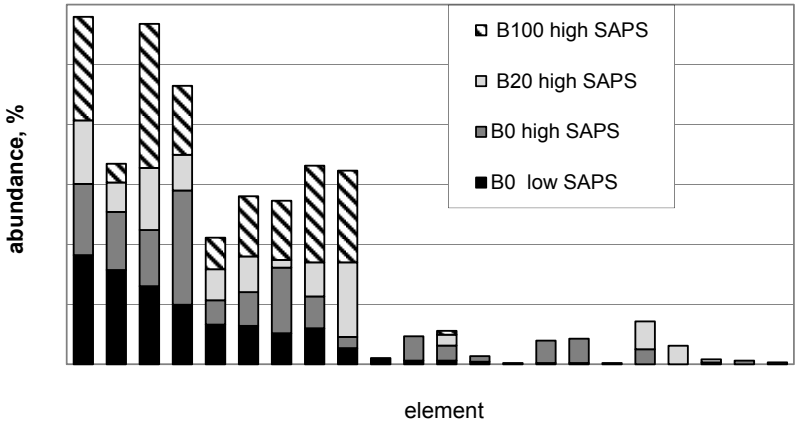

Fig. 3. Abundance of elements over individual particles in diesel B0 high and low SAPS, and biodiesel B20 and B100, high SAPS.

new specific Group Na, Cl, K-rich is found where marker elements of biofuel combustion Na, Cl, and K create the separate group and significantly contribute its overall composition. Representative micrographs for groups of B20 high SAPS are shown in Fig. 4. Abundance of Cl is significantly increased for biofuel emissions, Fig. 3. Because alkaline earth and alkali compounds are easily vaporized creating fumes under combustion conditions, at the exhaust cooling they may produce ultrafine particles externally mixed with others. Chlorine in these particles may exist in ion form, in accordance with ion measurements, Fig. 2, producing sodium and potassium chlorides. Group Zn- and W-bearing may also serve as micromarkers of high SAPS lube oil.

For biodiesel B100 when diesel fuel is completely replaced by biofuel we observe the group with K as dominant element at averaged concentration of 7 wt%. In accordance with well-recognized assignment of potassium to biomarker of biomass burning (Reid *et al.*, 2005) we may propose Group Na, Cl, K-rich in biodiesel exhaust as biomicromarker of biodiesel using. Elevated abundance of S over particles in B100 high SAPS demonstrates the impact of high ash content in lube oil relating to sulfates production, thus indicating Group S-bearing as micromarker of high SAPS lube oil in this exhaust.

Exhaust Toxicity

In our recent study of Steiner *et al.* (2013) in framework of the same measurement campaign the Opel engine exhaust was diluted then folds with heated filtered ambient air to expose a complex 3D cellular model of the human airway epithelium *in vitro* at the air-liquid interface. In parallel to exhaust exposures, identical cell cultures were exposed to filtered ambient air, which allows differentiating between exposure system and cell culture effects from purely exhaust. The cell cultures were exposed for 2 or 6 hrs to exhaust samples or filtered air followed by a 6 hrs post-incubation. An assessment was performed by toxicity tests of exposed cells, i.e., cytotoxicity, oxidative stress, and inflammation. Pro-inflammatory responses were assessed by quantification of the pro-inflammatory cytokines tumor necrosis factor *TNF-α* and interleukin *IL-8* by enzyme linked immune-sorbent assay (ELISA). A detailed discussion of toxicological findings is given elsewhere (Steiner *et al.*, 2013).

Here we perform the particle characterization study for the same engine operation conditions when cell exposure tests were done and no significant cytotoxic reactions found at different fuel and lube oil conditions. All exhausts induced considerable oxidative stress. The effect was weaker for B0 low SAPS in comparison with high SAPS. If particle properties in exhaust are the most important factor influencing the biological responses, we may relate micromarkers of contaminations in lube oil found for high SAPS exhaust to this effect because hydrophobic character of nonoxidized surface of diesel exhaust and undistinguishable difference in organic chemistry. Using pure fatty rapeseed methyl ester for B100 high SAPS leads to increasing the oxidative stress in comparison with B20 high SAPS, thus indicating the role of biofuel composition which may be associated with biomicromarkers found for biofuel exhausts as well with higher oxidation and nitrification of the biofuel particle surface, relating with higher reactivity and oxidation behavior.

Diesel/biodiesel exhausts are found capable of inducing pro-inflammatory responses, a finding dependent on the exposure duration and the pro-inflammatory marker under investigation. The highest induction of *TNF* gene expression is detected for B0 high SAPS (comparable for 2 and 6 hrs exposure), B100 high SAPS (6 hrs) and B0 low SAPS (6 hrs). Exposure to B20 high SAPS, B100 high SAPS (2 hours) and B0 low SAPS (2 hrs) exhaust did not induce *TNF* expression. A similar picture was obtained for *IL-8* gene expression (which is the biological downstream event of *TNF* expression): highest induction for B0 high SAPS, B100 high SAPS (6 hrs) and B0 low SAPS (6 hrs). Transcriptional induction of *IL-8* upon 2 hours of exposure to all tested exhaust types is lower than the one observed for B0 high SAPS and comparable to each other. In contrast to what is found for *TNF* gene expression, 6 hours exposure to B20 high SAPS clearly induce *IL-8* expression, even though to a lower extent than B0 high SAPS, B100 high

Table 2. Groups, abundance, averaged elemental composition (wt%) (upper line) with standard deviation (low line) for diesel B0 low SAPS particles.

Groups abundance %	C	N	O	F	Na	Mg	Al	Si	P	S	Cl	K	Ca	Ti	Mn	Fe	Ni	Pt
Soot 42,1	**79,9**	0,3	**13,5**	0,2	0,4	0,0	0,7	1,1	0,0	0,2	0,2	0,1	0,3	0,1	0,0	0,3	0,0	1,8
	17,4	3,2	11,6	2,0	1,6	0,1	2,2	2,6	0,0	0,7	0,6	0,6	1,1	1,4	0,0	1,7	0,0	10,5
Si-rich 21,5	15,0	0,0	50,5	0,0	0,5	0,4	1,1	**20,9**	0,0	0,1	0,0	4,4	0,5	0,1	0,1	6,5	0,0	0,0
	15,2	0,0	18,4	0,1	1,0	0,9	2,5	12,3	0,2	0,3	0,0	19,4	1,0	0,7	0,9	9,3	0,0	0,0
Fe- 21,5	14,2	0,0	27,7	0,0	0,0	0,0	0,0	0,9	0,0	0,0	0,0	0,0	0,3	0,0	0,0	**56,3**	0,5	0,0
	8,8	0,0	8,1	0,0	0,3	0,0	0,0	2,2	0,0	0,1	0,0	0,0	0,8	0,0	0,0	10,4	3,7	0,0
Ca-rich 8,7	33,7	0,0	39,1	0,0	0,0	0,3	0,0	0,1	0,2	1,3	0,0	0,0	**24,7**	0,0	0,0	0,6	0,0	0,0
	15,5	0,0	11,6	0,0	0,1	1,0	0,0	0,3	0,6	3,8	0,1	0,1	6,1	0,0	0,0	2,6	0,0	0,0
Al- 6,6	10,7	0,0	43,0	0,0	0,0	0,0	**46,3**	0,0	0,0	0,0	0,0	0,0	0,0	0,1	0,0	0,0	0,0	0,0
	9,4	0,0	6,2	0,0	0,0	0,0	4,0	0,0	0,0	0,0	0,0	0,0	0,0	0,2	0,0	0,0	0,0	0,0

SAPS or B0 low SAPS. Such complicated pro-inflammatory responses are not clear relating with structure of particle exhausts and their chemical composition, probably impact of gaseous emissions and exposure is also large. Intense research on how particle exhaust parameters change in response to fuel type, engine operation mode, exhaust after-treatment etc. and integration of such findings with toxicological results obtained by exposure of cell cultures may fill this gap in knowledge and to a certain extent may even allow for the prediction of exhaust toxicity based on exhaust characteristics.

CONCLUSIONS

Microscopic and chemical characterization of multicomponent diesel/biodiesel exhaust particles allows the quantification of major physico-chemical properties relating with morphology, elemental composition, organic/ inorganic content, and type of particles. The comprehensive analysis elucidates how combustion aerosols are changed in dependence on fuel and lube oil to reveal the general properties and distinguish the specific ones for diesel/biodiesel exhaust particles. Fuel additives, oil contaminations, and engine wear impact multicomponent aerosols composed of inorganic compounds (salts and metal oxides) emitted together with soot particles. Calcium, potassium, sodium combined with sulfates, chlorides, and nitrates compose inorganic salt compounds.

Chemical composition of diesel/biodiesel particles is dominated by aliphatic C-H groups in alkanes with relative low carbonyl C=O groups in carboxylic acids, ketones, aldehydes, esters, lactones, aromatic -NO_2 groups in nitrocompounds, and NO_3^- and SO_4^{2-} ions in inorganic salts. The relative concentration of carbonyl groups increases with the biodiesel fraction in the fuel, thus providing the increased surface hydrophilicity from hydrophobic for diesel B0 to the most hydrophilic for biodiesel B100. Hydrophobic character of nonoxidized surface of diesel exhaust is prominent and may determine the specific surface reactivity. More functionalized biodiesel particles may have a higher reactivity and show some oxidation behavior. The most developed functionalities are specific for biodiesel B100 particles with 100% of biofuel.

The diesel/biodiesel exhaust structure reveals the groups of carbonaceous and fly ash particles, in according the quantification of particle types in terms of physicochemical relevance. The most abundant group is typical soot agglomerates of mostly carbon and oxygen content at both diesel and biodiesel, low and high SAPS. Using high ash lube oil increases the abundance of metal (Nb, Zn, W) oxide and sulfur–containing groups while biodiesel fuel brings separate group with Na, K, and Cl biofuel markers. Thus, micromarkers discriminating between low and high ash-containing lube oil and the different types of fuels may be proposed. They could enable the classification of multicomponent aerosols according to diesel/biodiesel combustion source.

Individual particle analysis improves the characterization of multicomponent diesel/biodiesel particles for toxicological studies. The identification of morphological and

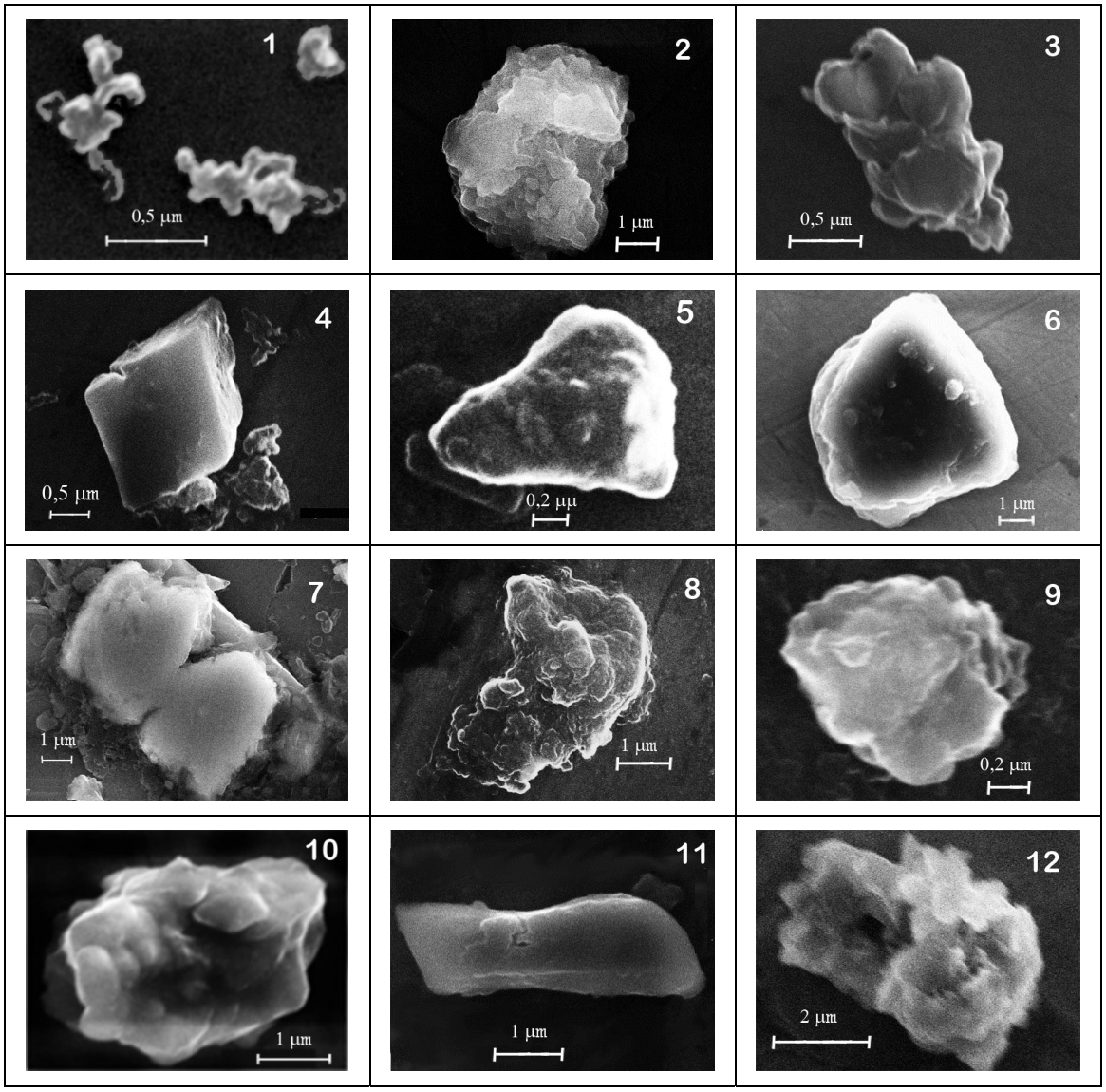

Fig. 4. Representative SEM micrographs of 1) soot, 2) Si-rich (aluminum silicate) and 3) Fe-bearing (iron oxide) particles, 4) Ca-rich (calcium sulfate), and 5) Al-bearing (aluminum oxide) particles in diesel B0 low SAPS in order of group abundance; 6) Si-rich (quartz), 7) Nb-bearing (niobium oxide), and 8) W- bearing (tungsten) particles in diesel B0 high SAPS; 9) Zn- bearing (zinc oxide), and 10) Na-rich (sodium chloride) in biodiesel B20 high SAPS; 11) Ca-rich (calcium oxide), and 12) K-rich (potassium chloride/sulfate) in biodiesel B100 high SAPS.

compositional micromarkers in emissions from combustion of fossil fuel and biofuels help elucidating toxicological properties of diesel exhaust under different combustion conditions. However, not all cellular reactions can be explained by those parameters due to possible large impact of gaseous exhaust. How exactly morphology, elemental composition, and organic/inorganic composition of exhaust particles translate into biological effects is not understood in detail so far.

ACKNOWLEDGMENTS

Financial support of Scientific & Technological Cooperation Programme, Switzeland-Russia, Université of Genève, from NSC-RFBR 12-05-92002 and RFBR 12-05-00395 projects, the Swiss Federal Office for the Environment, Erdölvereinigung EV and VSS lubes, as well as and the Adolphe Merkle Foundation is acknowledged.

REFERENCES

Bernstein, J.A., Alexis, N., Barnes, C., Bernstein, J.A, Nel, A., Peden, D., Diaz-Sanchez, D., Tarlo, S.M. and Williams, P.B. (2004). Health Effects of Air Pollution. *J. Allergy Clin. Immunol.* 114: 1116–1123.

Betha, R. and Balasubramanian, R. (2011). Particulate Emissions from Stationary Engine: Characterization and Risk Assessment. *Atmos. Environ.* 45: 5273–5281.

Bladt, H., Schmid, J., Kireeva, E., Popovicheva, O.B., Perseantseva, N.M., Timofeev, M.A., Heister, K., Uihlein,

J., Ivleva, N.P. and Niessner, R. (2012). Impact of Fe Content in Laboratory-produced Soot Aerosol on Its Composition, Structure and Thermo-chemical Properties. *Aerosol Sci. Technol.* 46: 1337–1348.

Chen, Y., Shah, N., Braun, A., Huggins, F.E and Huffman, G.P. (2005). Electron Microscopy Investigation of Carbonaceous Particulate Matter Generated by Combustion of Fossil Fuel. *Energy Fuels* 19: 1644–1651.

Chen, Y., Shah, N., Huggins, F.E. and Huffman, G.P. (2006). Microanalysis of Ambient Particles from Lexington, Ky, by Electron Microscopy. *Atmos. Environ.* 40: 651–663.

Chow, J.C., Yu, J.Z., Watson, J., Ho, S.S., Bohannan, T.L., Haysm, M.D. and Fung, K.K. (2007). The Application of Thermal Methods for Determining Chemical Composition of Carbonaceous Aerosols: A Rewiew. *J. Environ. Sci. Health., Part A* 42: 1521–1541.

Chow, J.C. and Watson, J.G. (2011). Air Quality Management of Multiple Pollutants and Multiple Effects. *Air Qual. Clim. Change* 45: 26–32.

Clague, A.D.H., Donnet, J.B., Wang, T.K. and Peng, J.C.M. (1999). A Comparison of Diesel Engine Soot with Carbon Black. *Carbon* 37: 1553–1565.

Coates, J. (2000). Interpretation of Infrared Spectra, a Practical Approach, In *Encyclopedia of Analytical Chemistry,* Meyers, R.A. (Ed.), John Wiley and Sons, Chichester, p. 10815–10837.

Cofala, J., Amann, M., Klimont, Z., Kupiainen, K. and Hoglund-Isaksson, L. (2007). Scenarios of Global Anthropogenic Emissions of air Pollutants and Methane Until 2030. *Atmos. Environ.* 41: 8486–8499.

Donaldson, K., Tran, C.L., Jimenez, L.A., Duffin, R., Newby, D.E. and Mills, N. (2005). Combustion-derived Nanoparticles: A Review of Their Toxicology Following Inhalation Exposure. *Part. Fibre Toxicol.* 2: 10–23.

Dwivedi, D., Agarwal, A.K. and Sharma, M. (2006). Particulate Emission Characterization of a Biodiesel vs Diesel Fuelled Compression Ignition Transport Engine: A Comparative Study. *Atmos. Environ.* 40: 5586–5595.

Geller, M.D., Ntziachristos, L., Mamakos, A., Samaras, Z., Schmitz, D.A. and Froines, J.R. (2006). Physicochemical and Redox Characteristics of Particulate Matter (PM) Emitted from Gasoline and Diesel Passenger Cars. *Atmos. Environ.* 40: 6988–7004.

Jung, H., Kittelson, D.B. and Zachariah, M. (2006), Characteristics of SMEBiodiesel-Fueled Diesel Particle Emissions and the Kinetics of Oxidation. *Environ. Sci. Technol.* 40: 4949–4955.

Kaniansky, D., Mazar, M., Marak, J. and Bodor, R. (1999). Capillary Electrophoresis of Inorganic Ions. *J. Chromatogr. A* 834:133–178.

Karavalakis, G., Boutsika, V., Stournas, S. and Bakeas, E. (2011). Biodiesel Emissions Profile in Modern Diesel Vehicles. Part 1: Effect of Biodiesel Origin on the Criteria Emissions. *Sci. Total Environ.* 409: 738–47.

Kireeva, E., Popovicheva, O., Persiantseva, N., Timofeyev, M. and Shonija, N. (2009). Fractionation Analysis of Transport Engine-Generated Soot Particles with Respect to Hygroscopicity. *J. Atmos. Chem.* 64: 129–147

Kleeman, M., Schauer, J. and Cass, J. (2000). Size and Composition Distribution of Fine Particulate Matter Emitted from Motor Vehicles. *Environ. Sci. Technol.* 34: 1132–1142.

Lighty, J.S., Veranth, J.M. and Sarofim, A.F. (2000). Combustion Aerosols: Factors Governing Their Size and Composition and Implications to Human Health. *J. Air Waste Manage. Assoc.* 50: 1565–1618.

Lin-Vien, D., Colthup, N.B., Fateley, W.G. and Grasselly, J.G. (1991). *The Handbook of Infrared and Raman Characteristic Frequencies of Organic Molecules,* Academic Press, Boston.

Maier, K.L., Alessandrini, F., Beck-Speier, I., Hofer, T.P.J., Diabatre, S., Bitterle, E., Stoger, T. and Jakob, T. (2008). Health Effects of Ambient Particulate Matter-Biological Mechanisms and Inflammatory Responses to in Vitroand in Vivo Particle Exposures. *Inhalation Toxicol.* 20: 319–337.

Mayer, A., Czerwinski, J., Ulrich, A., Wichser, A., Kasper, M. and Mooney, J. (2010). Metal-oxide Particles in Combustion Engine Exhaust. *SAE* 2010-01-0792.

Miller, A., Ahlstrand, G., Kittelson, D. and Zachariah, M. (2007). The Fate of Metal (Fe) During Diesel Combustion: Morphology, Chemistry, and Formation Pathways of Nanoparticles. *Combust. Flame* 149: 129–143.

Muller, L., Comte, P., Czerwinski, J., Kasper, M., Mayer, A., Gehr, P., Cher, H., Morin, J.P., Konstandopoulos, A. and Rothen-Rutishauser, B. (2010). New exposure System to Evaluate the Toxicity of (Scooter) Exhuast Emissions in Lung Cells in Vitro. *Environ. Sci. Technol.* 44: 2632–2638.

Oberdorster., G., Maynard A., Donaldson, K., Castranova, V., Fitzpatrick, J., Ausman, K., Carter, J., Karn, B., Kreyling, W., Lai, D., Olin, S., Monteiro-Riviere, N., Warheit, D. and Yang, H. (2005). Principles for Characterizing the Potential Human Health Effects from Exposure to Nanomaterials: Elements of a Screening Strategy. *Part. Fibre Toxicol.* 2: 8, doi: 10.1186/1743-8977-2-8.

Popovicheva, O.B., Persiantseva, N.M., Kuznetsov, B.V., Rakhmanova, T.A., Shonija, N.K., Suzanne, J. and Ferry, D. (2003). Microstructure and Water Adsorbability of Aircraft Combustor and Kerosene Flame Soots: Toward an Aircraft Generated Soot Laboratory Surrogate *J. Phys. Chem.* 107: 10046–10054.

Popovicheva, O.B., Kireeva, E.D., Shonija, N.K. and Khokhlova, T.D. (2009a). Water Interaction with Laboratory-simulated Fossil Fuel Combustion Particles. *J. Phys. Chem. A* 113: 10503–10511.

Popovicheva, O., Kireeva, E., Shonija, N., Zubareva, N., Persiantseva, N., Tishkova, V., Demirdjian, B., Moldanová, J. and Mogilnikov, V. (2009b). Ship Particulate Pollutants: Characterization in Terms of environmental Implications. *J. Environ. Monit.* 11: 2077–2086.

Popovicheva, O., Kireeva, E., Persiantseva, N., Timofeev, M., Bladt, H., Ivleva, N., Niessner, R. and Moldanová, J. (2012). Microscopic Characterization of Individual Particles from Multicomponent Ship Exhaust. *J. Environ. Monit.* 14: 3101–3110.

Reid, J., Koppmann, R., Eck, T. and Eleuterio, D.P. (2005). A Review of Biomass Burning Emissions Part II.

Intensive Physical Properties of Biomass Burning Particles. *Atmos. Chem. Phys.* 5: 799–825.

Rothen-Rutishauser, B., Blank F., Mühlfeld, C. and Gehr, P. (2008). In Vitro Models of the Human Epithelial Airway Barrier to Study the Toxic Potential of Particulate Matter. *Expert Opin. Drug Metabol. Toxicol.* 4: 1075–1089.

Sakurai, H., Tobias, H.J., Park, K., Zarling, D., Docherty, K., Kittelson, D.B., McMurry, P.H. and Ziemann, P.J. (2003). On-line Measurements of Diesel Nanoparticle Composition and Volatility. *Atmos. Environ.* 37: 1199–1210.

Singh, B.R. and Singh, O. (2012). Fossil Fuel and the Environment, Khan, S. (Ed.). Ch. 8: 167–192, InTech.

Steiner, S., Czerwinski, J., Comte, P., Popovicheva, O.B, Kireeva, E., Mueller, L., Heeb, N., Mayer, A., Fink, A. and Rothen-Rutishauser, B. (2013). Comparison of the Toxicity of Diesel Exhaust Produced by Bio- and Fossil Diesel Combustion in Human Lung Cells in Vitro. *Atmos. Environ.* 81: 380–388.

Steiner, S., Muller, L., Popovicheva, O.B, Raemy, D.O, Czerwinski, J., Comte, P., Mayer, A., Gehr, P., Rothen-Rutishauser, B. and Clift, M.J.D. (2012). Cerium Dioxide Nanoparticles Can Interfere with the Associated Cellular Mechanistic Response to Diesel Exhaust Exposure. *Toxicol. Lett.* 214: 218–225.

Su, D., Serafino, A., Muller, J.O., Jentoft, R.E., Schlogl, R. and Fiorito, S. (2008). Cytotoxicity and Inflammatory Potential of Soot Particles of Low-emission Diesel Engines. *Environ. Sci. Technol.* 42: 1761–1765.

Toner, S.M., Sodeman, D.A. and Prather, K.A. (2006). Single Particle Characterization of Ultrafine and Accumulation Mode Particles from Heavy Duty Diesel Vehicles Using Aerosol Time-of-flifgt Mass Spectrometry. *Environ. Sci. Technol.* 40: 3912–3921.

Topinka, J., Milcova, A., Schmuczerove, J., Mazac, M. and Pechout, M. (2012). Genotoxic Potential of Organic Extracts from Particles Emissions of Diesel and Rapeseed Oil Powered Engines. *Toxicol. Lett.* 212: 11–17.

Vander Wal, R., Yezerets, A., Currier, N.W., Kim, D.H. and Wang, C.M. (2007). HRTEM Study of Diesel Soot Collected from Diesel Particulate Filters. *Carbon* 45: 70–77.

Vester, B., Ebert, P., Barnert, E.B., Schneider, J., Kandler, K., Schütz, L. and Weinbruch, S. (2007), Composition and Mixing State of the Urban Back Ground Aerosol in the Rhein-Main Area (Germany). *Atmos. Environ.* 41: 6102–6111.

Wang, Y.F., Huang, K.L., Li, C.T, Mi, H.H., Luo, J.H. and Tsai, P.J. (2003). Emissions of Fuel Metals Content from a Diesel Vehicle Engine. *Atmos. Environ.* 37: 4637–4643.

Received for review, November 15, 2013
Accepted, March 6, 2014